JOURNAL OF MATERIALS SCIENCE 28 (1993) 4918–4924

Investigation of microstructure of mechanically alloyed TiMo particles using high-resolution electron microscope observations

E. SUKEDAI
Faculty of Engineering, Okayama University of Science, Okayama 700, Japan
W. Y. LIM, M. HIDA*
*Graduate School, and *Faculty of Engineering, Okayama University, Okayama 700, Japan*

Mechanically alloyed TiMo alloy particles were evaluated by high-resolution electron microscope observations. The particles were mechanically alloyed for 36, 72, 144 and 288 ks. Specimens for transmission electron microscopy were prepeared by electroplating the particles together with nickel on copper sheets and using an ion-milling machine. It was not difficult to distinguish MA particles in the specimens. MA particles consisted of small island crystalline parts, 20–50 nm diameter, and amorphous parts. Lattice fringes of island crystalline parts were measured and the materials produced by mechanical alloying were identified by their lattice spacings. After alloying for 36 ks, pure titanium and molybdenum still remained and a small amount of β-TiMo alloy was confirmed. After alloying for 72 ks, almost all crystalline parts were β-TiMo alloy. α-TiMo and TiFe were found after alloying for 144 ks. α-TiMo alloy seems to be transformed from β-TiMo alloy on alloying for 144 and 288 ks.

1. Introduction

Mechanical alloying is a method of synthesis for various materials using a solid-state reaction, namely repeated cold welding, friction, fracture and their interactions with powder particles [1, 2]. It also appears that this method has a significant advantage over some other alloying methods, which have been used so far, in which alloying elements are melted together and cooled in various ways. In those processes, the solubility of the solvent is limited, and hence it seems that the production of new materials is limited when using these methods. However, a mechanical alloying method has no such limitation, because the production of alloys with a wide range of compositions seems to be possible using this method. Recently, the production of some alloys has been attempted by this method [1–6], and their physical and chemical properties have been investigated by X-ray [2, 4, 5], DSC [5, 6], SEM [3, 5] and electron diffraction [7] methods. However, it appears to be very important that the microstructure of mechanically alloyed (MA) particles is investigated using transmission electron microscopy, especially at the atomic level, because the microstructure of alloys generally determines their important properties. Various attempts at specimen preparation for transmission electron microscope observation have been made; MA particles were set in resin and then sliced using a microtome with a diamond knife [7], MA particles were dispersed in alcohol and scooped out on a microgrid after setting of large MA particles [8]. Moreover, as a simple case of MA processing, a thin foil was prepared by rolling two kinds of metal sheets 20 times [9]. However, it has been greatly hoped that every size of MA particle could be observed without any damage occurring during the specimen preparation. We have developed a new method by which to prepare a specimen of MA TiMo alloy particles for transmission electron microscopy (TEM) using nickel plating [10].

In the present paper, specimens of TiMo alloy particles mechanically alloyed for 36, 72, 144 and 288 ks were prepared by this method and observed using high-resolution electron microscopy. Some results are discussed.

2. Experimental procedures

Elemental powders of titanium and molybdenum used in this work were weighted in the ratio of Ti–14 mass % Mo and mixed in a glove box filled with purified argon gas. The mixture was filled in a stainless steel vessel of a high-energy ball mill (Mitui Miike attritor MAID, Japan) under a purified argon atmosphere, in which stainless steel balls of 9.53 mm diameter, 171.5 N total weight, were packed. Mechanically alloyings were performed for 36, 72, 144, and 288 ks. The rotational speed of the arms was 300 r.p.m.

Fig. 1 shows a schematic diagram of the preparation method of the TEM specimen. The anode was a pure nickel plate, 0.1 mm thick, and the cathode was a pure copper sheet 35 μm thick. The size of both electrodes was 20 mm × 20 mm. The composition of the electrolyte was a 4.10:0.059:0.309 (by newton in 1000 ml[3]

0022–2461

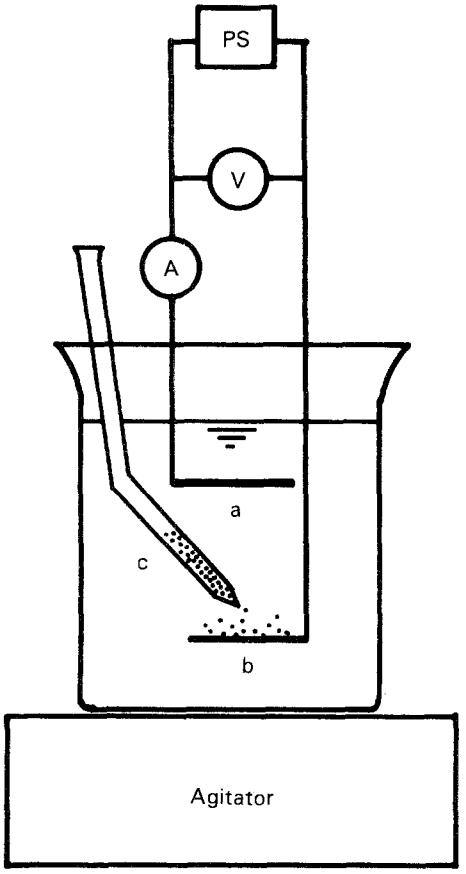

Figure 1 Schematic diagram of the specimen preparation method of MA particles for TEM. a, nickel anode; b, copper cathode; c, glass tube for supplying MA particles.

water) solution of $Ni(NH_2SO_3)_24H_2O$:$NiCl_6H_2O$:H_3BO_3. The conditions of nickel electroplating were a voltage of 3 V and a current density of 45 mA cm^{-2} at about 300 K. During electroplating, MA particles about 0.03 N were supplied continuously to the copper foil and were electroplated together with nickel. Supplying MA particles began after the thickness of the nickel layer reached > 10 μm and ended when the thickness was about 60 μm. After finishing the electroplating, the copper foil was mechanically removed and the nickel sheet, including MA particles, was cut into a disc, 3 mm diameter, using a spark erosion machine. The disc was dimpled using a dimpling machine (Dimpler D-500) to 30 μm thick and thinned with an ion-milling machine until a small hole was opened. MA particles in the electroplated nickel sheet were surveyed using an optical microscope and electron probe microanalyser (EPMA). The specimens prepared using this method with MA particles for each period were observed using JEM-4000EX operated at 400 kV at the atomic level.

3. Results and discussion

3.1. Evaluation of specimen preparation

Fig. 2 shows an optical micrograph of a cross-section of an electroplated nickel sheet involving MA particles. The existence of many MA particles can be seen. Fig. 3a shows a scanning electron micrograph of a disc specimen. The white area on the left is the specimen and the area outlined by the white line (denoted

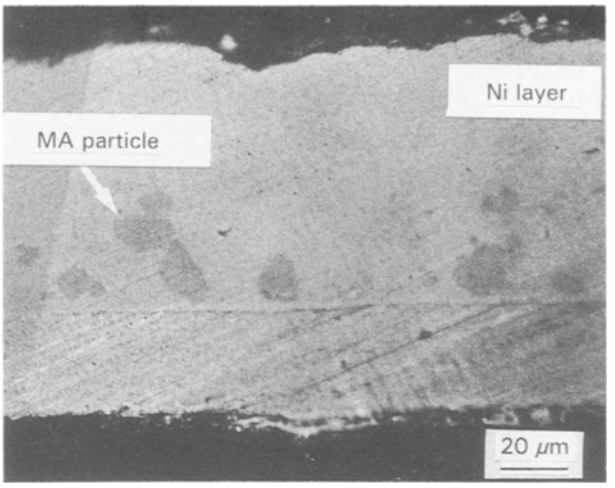

Figure 2 Optical micrograph of a cross-section of an electroplated nickel sheet containing MA particles.

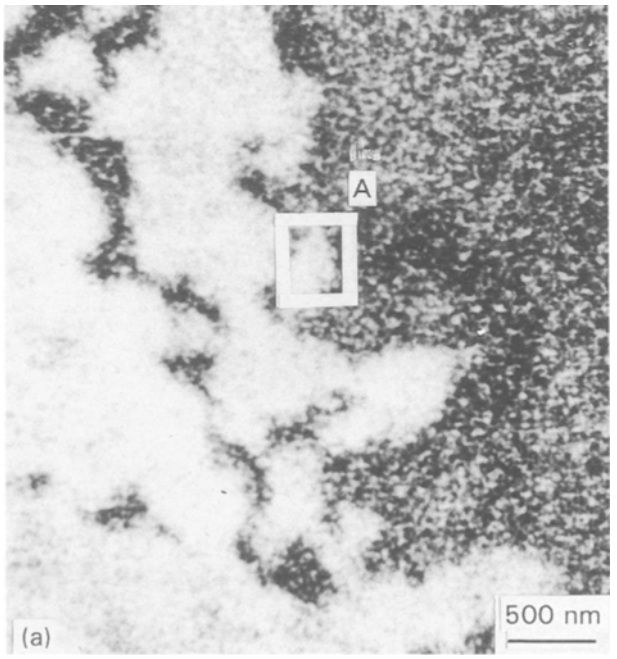

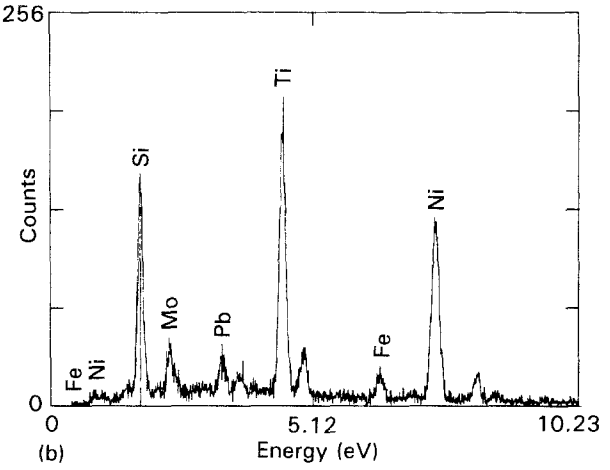

Figure 3 (a) SEM image of a TEM specimen, and (b) EPMA spectrum of the area outlined by white lines in (a).

A) was analysed by EPMA. Fig. 3b shows the result. Because titanium and molybdenum peaks can be seen, it is deduced that in area A, an MA particle was included in an electroplated nickel sheet. A silicon

peak was observed from the specimen holder. An iron peak was also observed, apparently due to the mixing from the balls, arms and wall of the vessel during MA processing, as described in a previous paper [8].

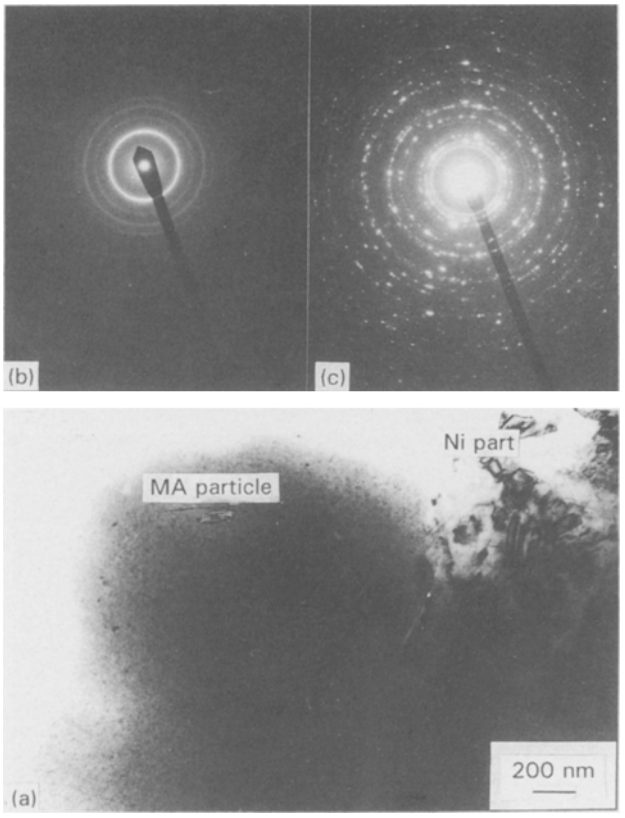

Figure 4 (a) TEM image near the boundary between an MA particle and an area of nickel. (b) SAD pattern of the MA particle. (c) SAD pattern of the nickel layer.

Fig. 4 shows a bright-field image near the boundary between an MA particle and an electroplated nickel sheet in a specimen. The MA particle image was not clear and small island crystalline parts, about 20 nm diameter, can be seen. The diffraction pattern of the MA particle was small diffuse rings. On the other hand, the image of the nickel layer was clear, and dislocations and bend contours can be seen. The diffraction patterns also showed spotty-rings. Hence, it was not very difficult to distinguish both parts by electron microscope observation.

3.2. Diffraction patterns from particles mechanically alloyed for various periods

Fig. 5 shows selected-area diffraction (SAD) patterns from the particles mechanically alloyed for each period. Fig. 5a shows an SAD pattern for 36 ks. Three rings and weak halo rings can be seen and corresponding to (1 0 $\bar{1}$ 0), (1 0 $\bar{1}$ 1) and (1 1 $\bar{2}$ 0) of α-Ti. The lattice spacings of α-Ti were calculated using lattice parameters of pure titanium. The inner halo ring seems to be at the position of (1 1 0) of β-TiMo alloy. In this work, the lattice spacings of α-TiMo and β-TiMo were identified using the data of Ti–15% Mo alloy [11]. The halo rings seem to suggest the existence of an amorphous region. It is noted that no solid solution was produced in this stage. This result seems to agree with that obtained by X-ray diffraction analysis [6]. Fig. 5b shows an SAD pattern for 72 ks. It was found that the halo ring at the position of (1 1 0) of β-TiMo alloy became stronger than that in Fig. 5a. Thus it seems that the amorphous regions increased and

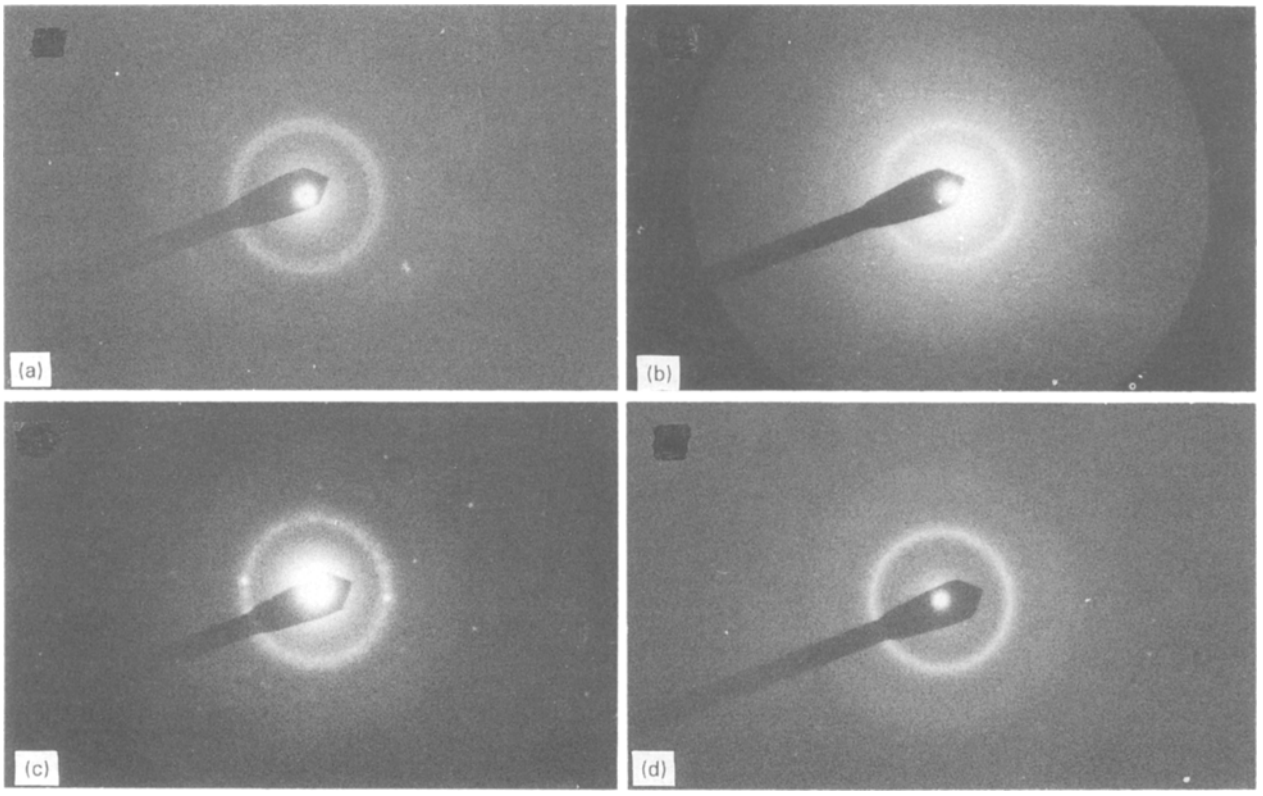

Figure 5 SAD patterns of particles mechanically alloyed for (a) 36 ks, (b) 72 ks, (c) 144 ks and (d) 288 ks.

β-TiMo alloy was formed. Fig. 5c shows an SAD pattern for 144 ks and some spots can be seen in the halo ring. The appearance of these spots suggests that a certain part of the β-TiMo alloy transforms to α-TiMo and/or an intermetallic compound TiFe (see Section 3.3). In the latter case, iron atoms seem to be dissolved from the balls, arms and wall of the vessel. However, these spots disappeared after mechanically alloying for 288 ks, as shown in Fig. 5d. It can be seen that the diffraction ring completely becomes a halo. Because the results of X-ray diffraction analysis of the particles at this stage showed that many iron atoms were mixed into the particles from the apparatus, it appears that iron atoms promote production of amorphous parts [12].

3.3. HREM images of the particles mechanically alloyed for each period

Because MA particles were made up of small island crystalline and amorphous parts, as shown in Fig. 4, it is useful in considering the detail of MA particles, to observe their atomic structure. Fig. 6 shows a high-resolution image of a particle mechanically alloyed for 36 ks and lattice fringes of (1 0 $\bar{1}$ 0), (1 0 $\bar{1}$ 2) and (0 0 0 2) of α-Ti, (1 1 0) of β-Mo and (1 1 0) of β-TiMo alloy can be identified. It is also found that MA particles are divided into many small island crystals of about 20–50 nm diameter. Among these crystals, the regions without lattice fringes were observed. In all MA particles for each stage of this work, those regions were observed, and they will be discussed later.

Fig. 7 shows an HREM image of a particle mechanically alloyed for 72 ks, and lattice fringes of (1 1 0) and (2 0 0) of β-TiMo alloy were observed. Another image, taken from MA particles in this stage, showed only fringes of β-TiMo alloy. It is noted that the amount β-TiMo alloy produced was considerable in this stage.

Fig. 8 shows an HREM image of a particle mechanically alloyed for 144 ks, and lattice fringes of (1 1 0) of β-TiMo alloy, (1 1 $\bar{2}$ 0) of α-TiMo alloy and (1 1 0) of intermetallic compound TiFe can be seen. Because α-TiMo alloy was observed in this particle, it appears that some parts of β-TiMo alloy crystals formed in an earlier stage were transformed to α-TiMo alloy during MA processing. The transformation from β-TiMo to α-TiMo alloy has been reported in TiMo alloy [13]. It also appears that the compound TiFe was produced by the reaction of titanium and impurity iron.

Fig. 9 shows an image of a 288 ks MA particle, and lattice fringes of (1 1 0) of β-TiMo alloy, (1 0 $\bar{1}$ 1) of α-TiMo alloy and (1 1 0) of intermetallic compound TiFe can be seen. It was found that the quantities of α-TiMo alloy and the intermetallic compound TiFe increased.

An investigation of the region without the lattice fringes mentioned above, was carried out by two

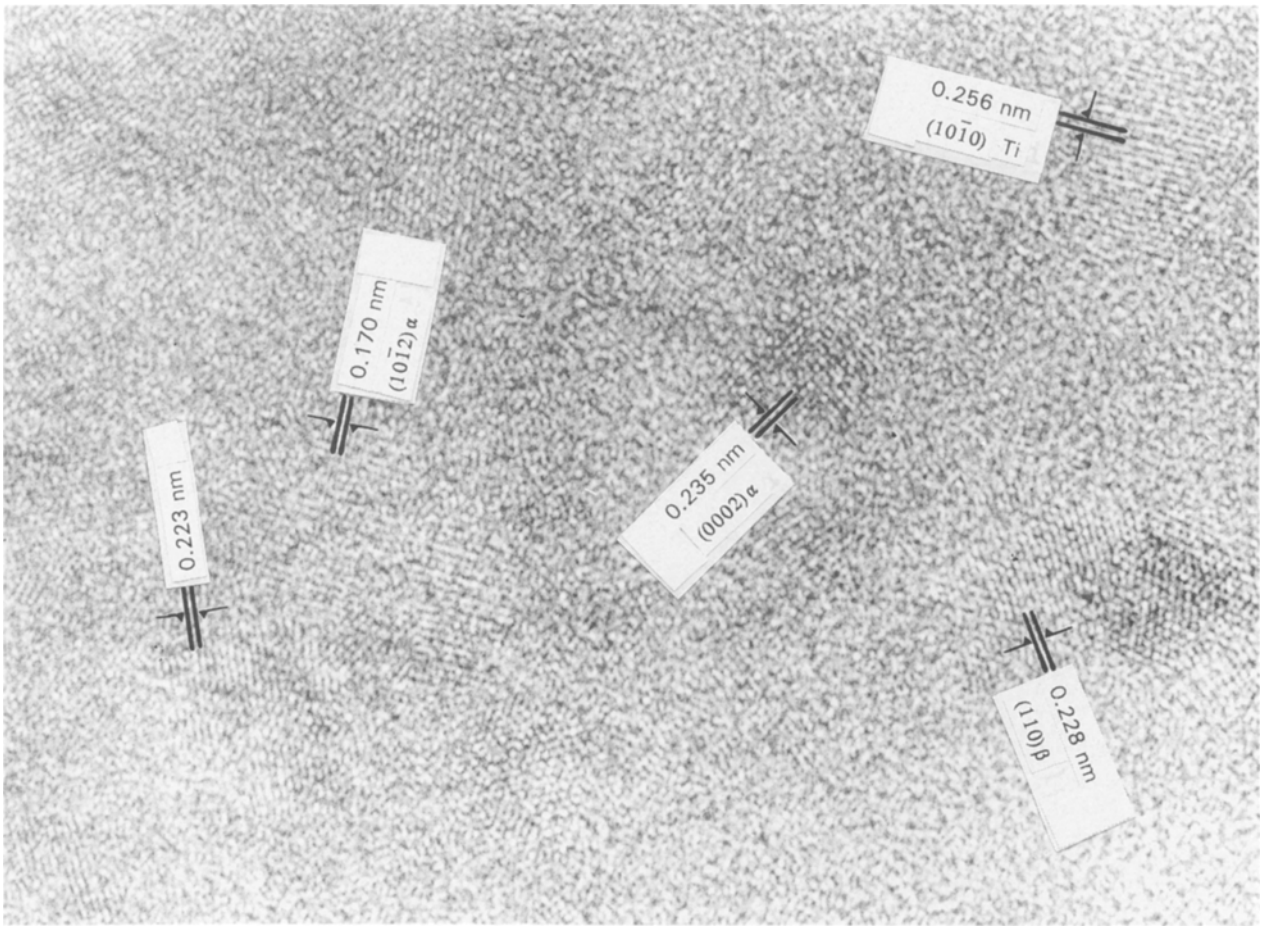

Figure 6 An HREM image of a particle MA for 36 ks.

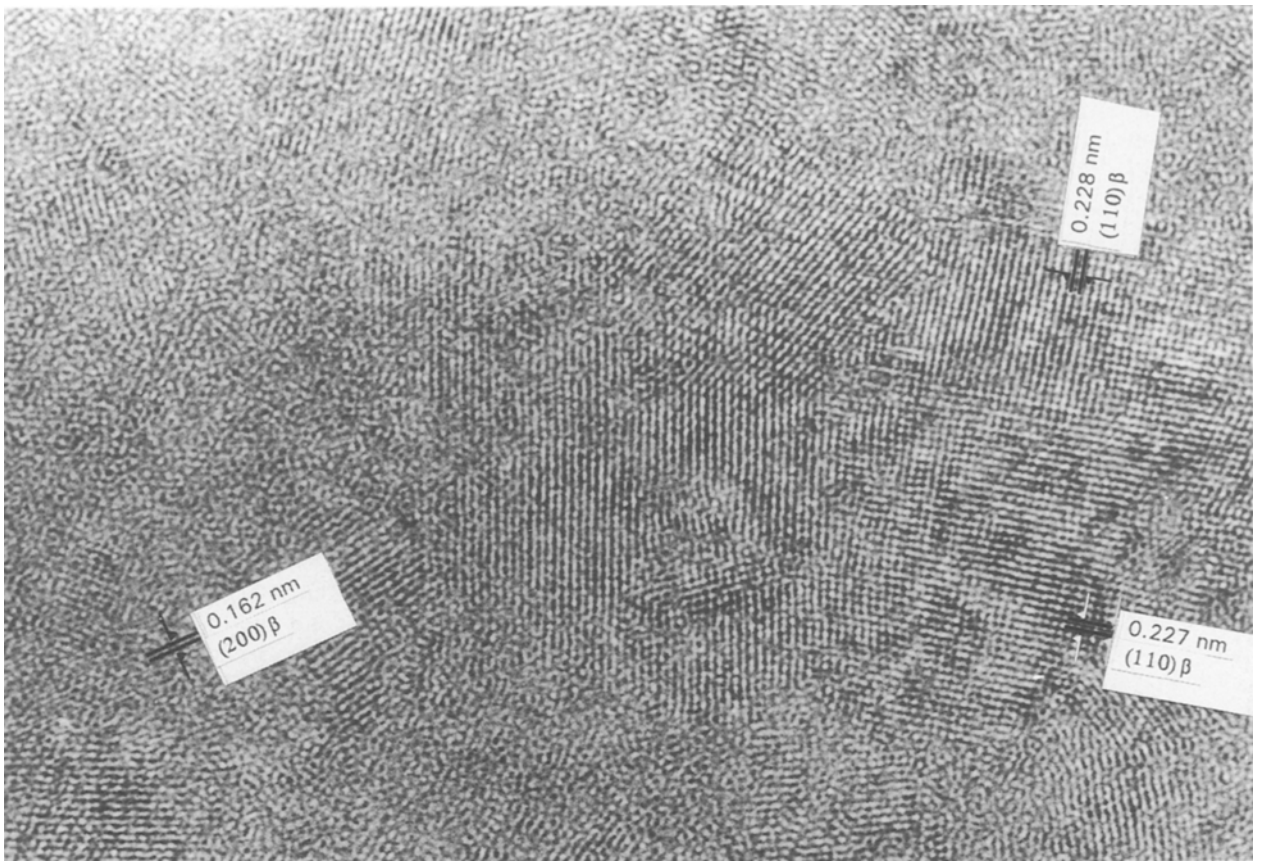

Figure 7 An HREM image of a particle MA for 72 ks.

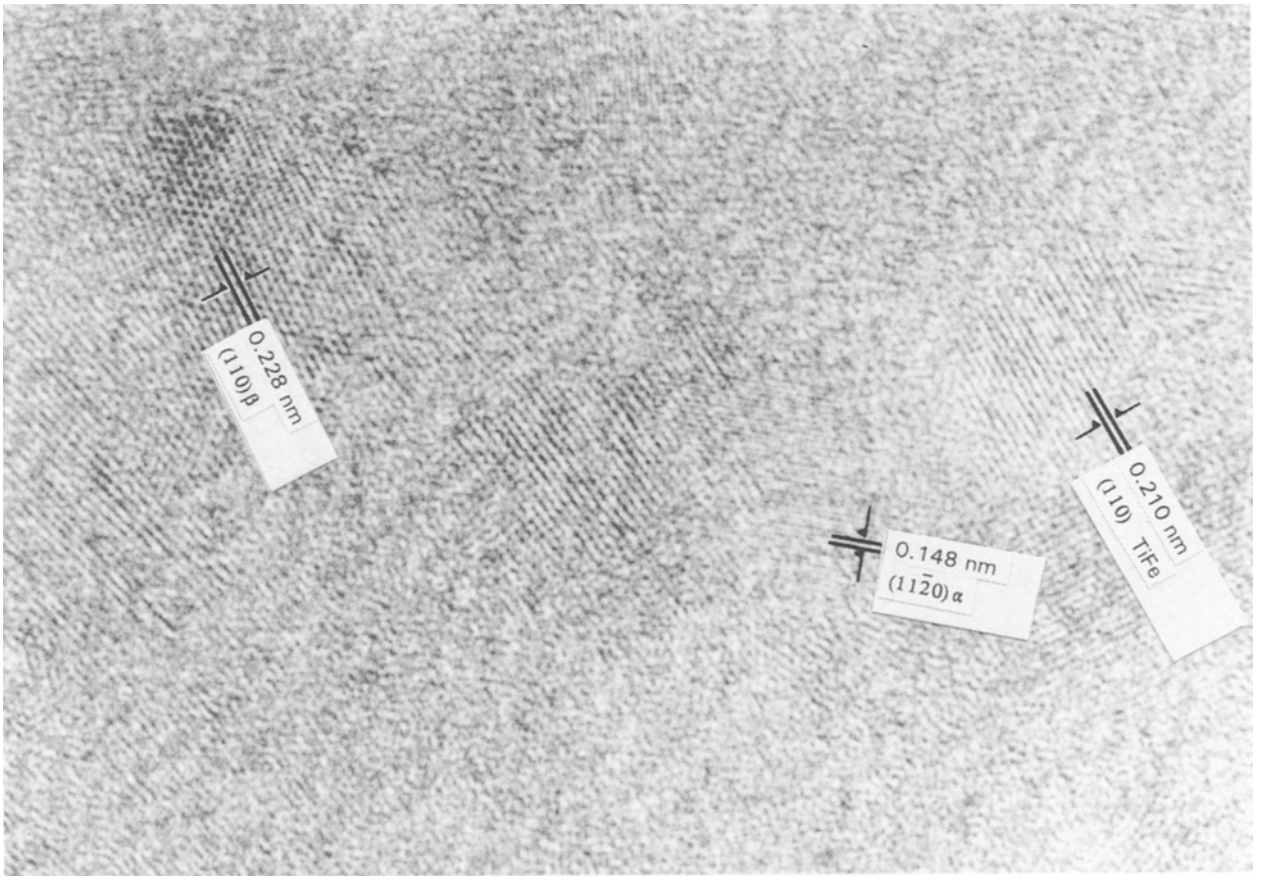

Figure 8 An HREM image of a particle MA for 144 ks.

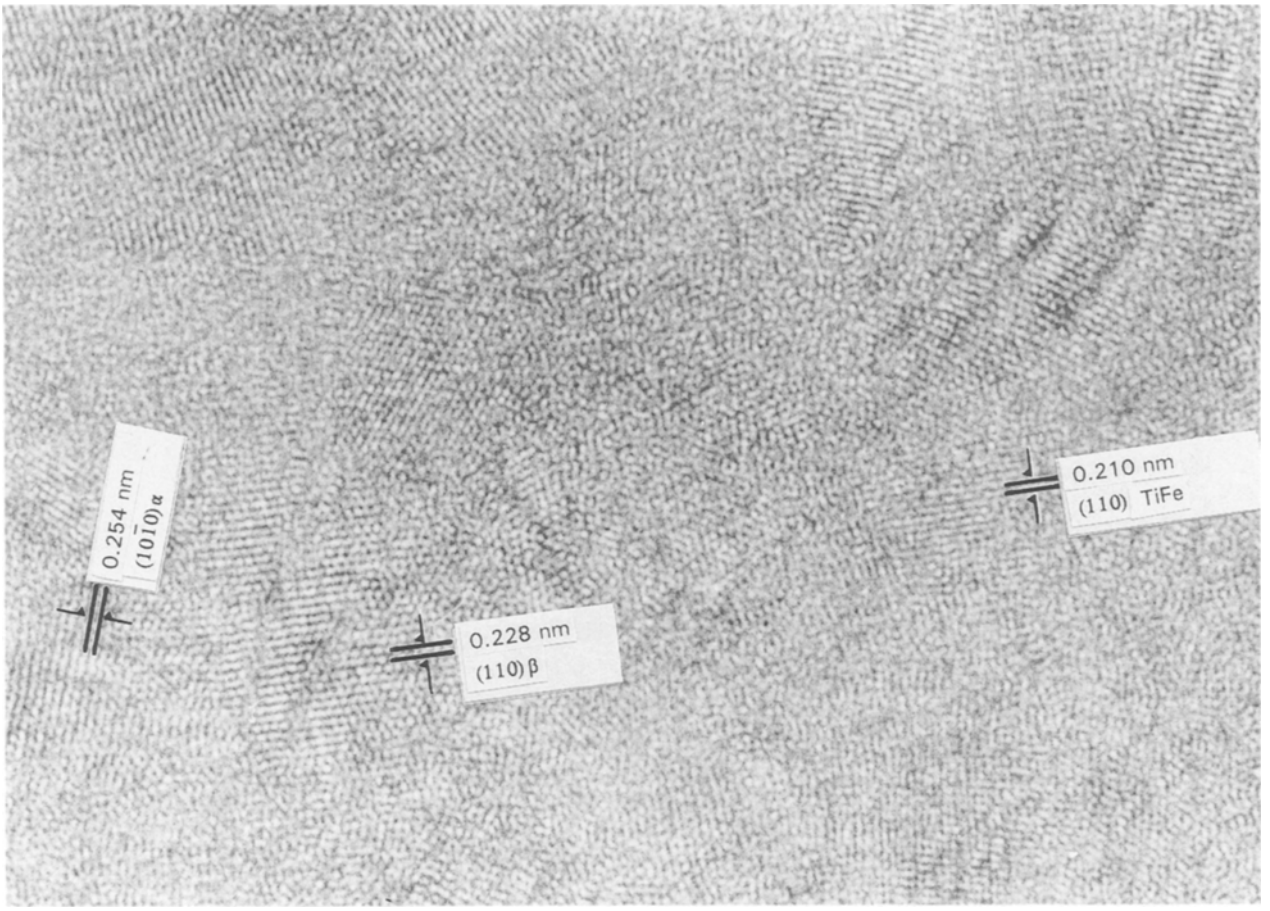

Figure 9 An HREM image of a particle MA for 288 ks.

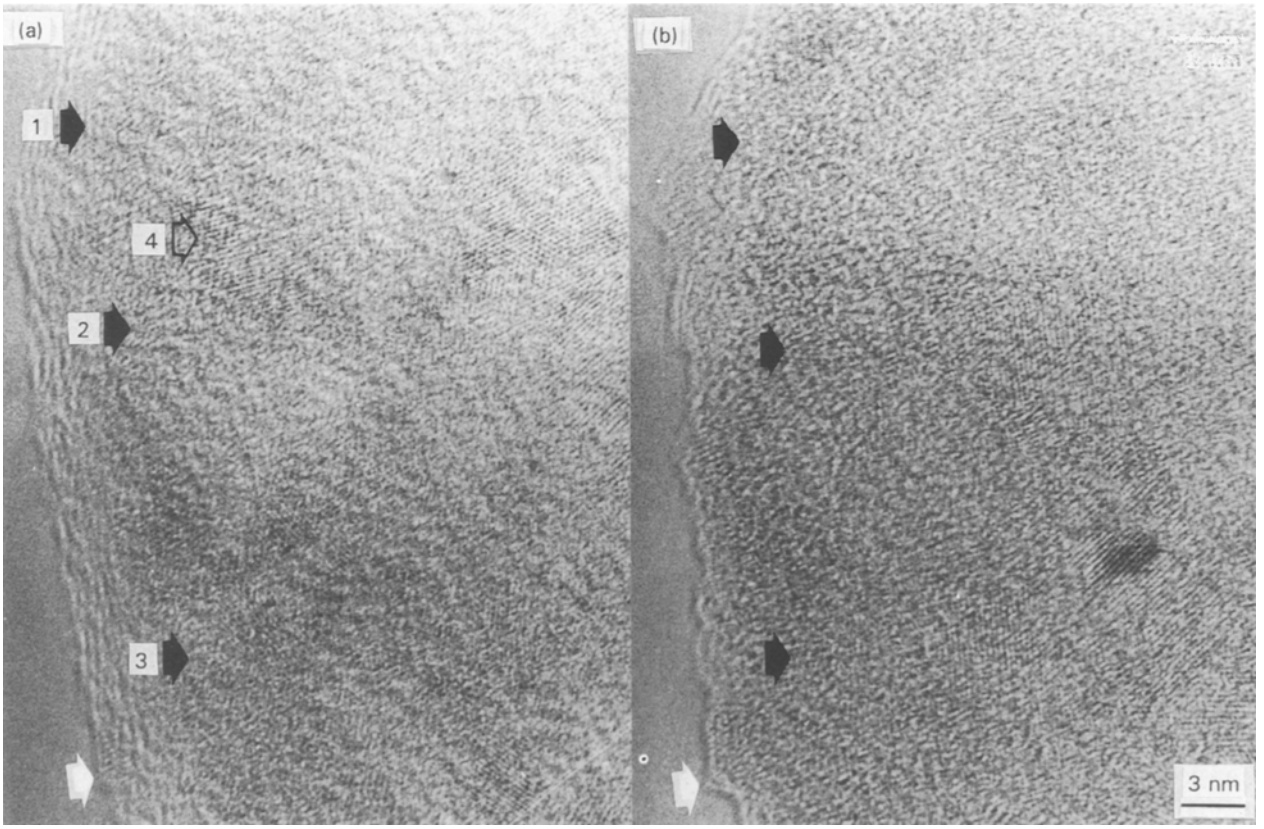

Figure 10 HREM images of the same area of a particle MA for 144 ks: (a) was tilted by 9° with respect to (b). The regions indicated by arrows 1, 2, 3 seem to be amorphous. The region indicated by arrow 4 seems to be crystalline.

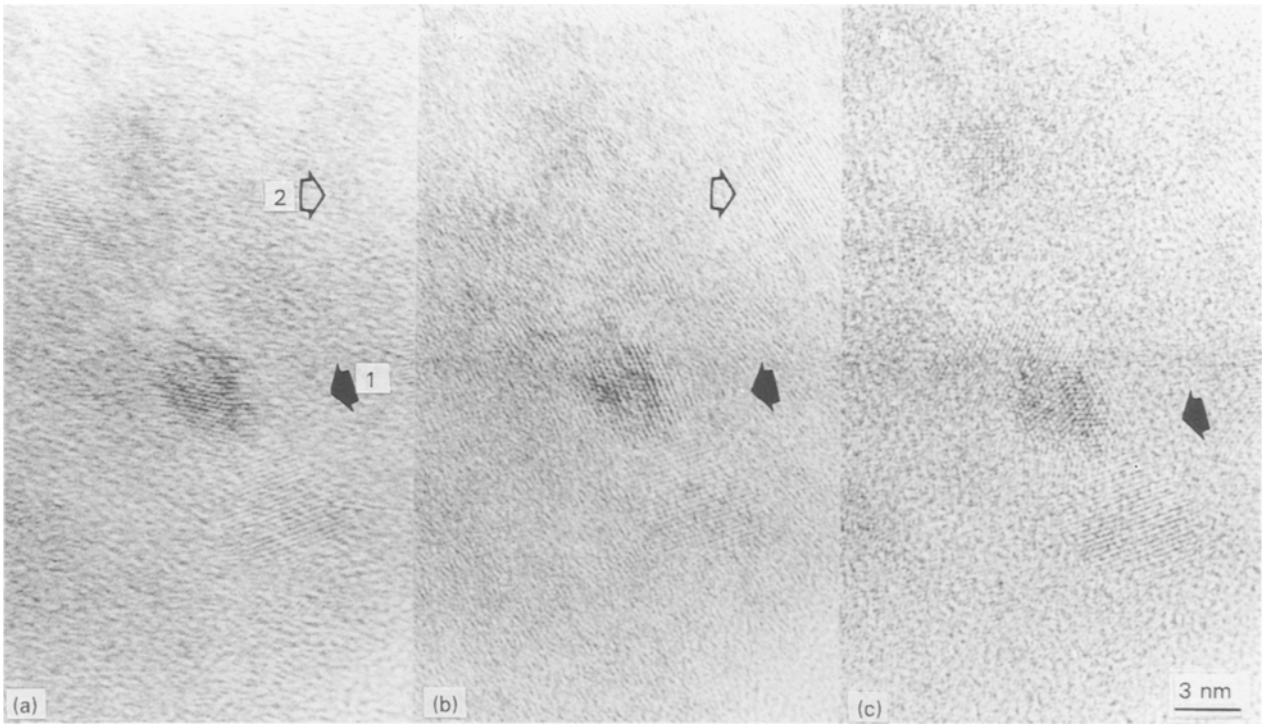

Figure 11 HREM images of the same area of a particle MA for 36 ks with different defocus values: (a) 14 nm, (b) − 56 nm and (c) − 53 nm. The region indicated by arrow 1 seems to be amorphous, whereas the region denoted by arrow 2 seems to be crystalline.

different methods. One was by tilting the specimen with respect to the incident beam. Fig. 10a and b show the images obtained by this method; the tilting angle between the two images was 9°. In these images, white arrows indicate the same point on the specimen. It was found that in the regions indicated by black arrows 1, 2 and 3, lattice fringes could not be seen in either image, hence these regions seem to be amorphous. In Fig. 10b, at the regions indicated by black arrow 4, lattice fringes did not appear, however, due to the tilting, lattice fringes appear, hence this region is a crystalline part. The second method was by changing the defocus values of the electron microscope. Fig. 11a–c show the results; the defocus values were 14 nm in (a), − 56 nm in (b) and − 53 nm in (c). In the regions indicated by arrow 1, lattice fringes could not be seen in any of the three images, hence this region seems to be amorphous. At the region indicated by arrow 2, lattice fringes could not be seen in Fig. 11a; however, lattice fringes did appear in Fig. 11b and c. It seems that in this region crystalline and amorphous parts were overlapped. It was also noted that the tilting method was useful for determining whether or not the region was crystalline or amorphous.

4. Conclusions

1. Because it is not very difficult to distinguish mechanically alloyed particles prepared by a new method developed for TEM specimens using transmission electron microscopy, it was found that this new preparation method was very useful for TEM observation of MA particles.

2. Using high-resolution electron microscope observations it was found that mechanically alloyed particles consisted of small island crystalline parts (20–50 nm diameter) and amorphous ones.

3. Materials produced by the mechanical alloying process for each period could be identified using measurement of lattice fringes, and it was found that these results agreed with those from X-ray diffractometry.

Acknowledgement

The authors thank Mr K. Kaneko, undergraduate student, Okayama University of Science, for his help in preparing TEM specimens.

References

1. J. S. BENJAMIN, *Sci. Amer.* **234** (1976) 40.
2. R. B. SCHWARZ and C. C. KOCH, *Appl. Phys. Lett.* **49** (1986) 146.
3. R. B. SCHWARZ, *Mater. Sci. Engng* **97** (1988) 71.
4. E. HELLSTERN and L. SCHULTZ, *Appl. Phys. Lett.* **48** (1986) 124.
5. R. B. SCHWARZ, R. R. PETRICH and C. K. SAW, *J. Non Cryst. Solids* **76** (1985) 281.
6. W. Y. LIM, M. HIDA, A. SAKAKIBARA, E. SUKEDAI and Y. NAKANO, *J. Jpn Inst. Metals* **55** (1991) 125.
7. P. TLOMAK, S. J. PIERZ, L. J. PAULSON and W. E. BROWER, *Mater. Sci. Engng* **97** (1988) 369.
8. W. Y. LIM, M. HIDA, A. SAKAKIBARA, Y. TAKEMOTO, H. MAEDA and E. SUKEDAI, *J. Jpn Soc. Powder Powder Mater.* **37** (1990) 636.
9. H. SHINGU, *J. Jpn Inst. Light Metals* **40** (1990) 850.
10. W. Y. LIM, E. SUKEDAI, M. HIDA and K. KANEKO, *Mater. Sci. Forum* **88–90** (1992) pp. 105–109.
11. R. M. WOOD, *Acta Metall.* **11** (1963) 907.
12. S. H. LOUR and C. L. CHIEN, *Phys. Rev. B* **35** (1987) 2443.
13. S. TERAUCHI, H. MATSUMOTO, T. SUGIMOTO and K. KAMEI, *J. Jpn Inst. Metals* **41** (1977) 632.

Received 21 January
and accepted 20 November 1992